CrystEngComm

Accepted Manuscript

ROYAL SOCIETY OF CHEMISTRY

www.rsc.org/crystengcomm

Journal Name

COMMUNICATION

Controllable synthesis of rutile titania with novel curved surfaces

Hanglong Wu, ‡ Hengbo Li, ‡ Jun Li, Bin Lu, Yueke Yang, Wentao Yuan, Yong Wang* and Ze Zhang

Received 00th January 20xx,
Accepted 00th January 20xx

DOI: 10.1039/x0xx00000x

www.rsc.org/

We report a facile organic-free hydrothermal strategy to fabricate rutile TiO_2 single crystals with a new type of curved surfaces, which consist of high-energy-facet-bound nano-hills rather than quasi-continuous miller-index microfacets. Moreover, by solely altering the concentration of F^-, the proportion of facets as well as the aspect ratio of TiO_2 could be readily controlled.

Sustained efforts have been made in the synthesis of functional inorganic semiconducting oxides with a variety of shapes and exposed high-energy facets[1-8], which are demonstrated strongly influencing the performance in catalysis[1, 4, 5], sensing[7], and many other surface-enhanced applications of semiconducting oxide crystals. In addition to those bound by common flat facets, crystals with curved surfaces, which usually exhibit distinct properties[9], are also ubiquitous in nature, such as viral capsids, pollen grain, calcitic skeleton etc. Nevertheless, up to now, few studies have been reported on synthesizing semiconducting functional materials with unique curved surfaces, including titanium dioxide (TiO_2), one of the most important semiconductors. In the past five years, TiO_2 crystals with tailored facets have been one of the hottest research topics[2], and various facets have been achieved through different synthetic strategies[1,10-18]. Very recently, Yang and coworkers[9] did a pioneering work that they successfully synthesized TiO_2 single crystals with curved surfaces using organic acid and hydrofluoric acid (HF) as synergistic capping agents and moreover, they found that organic agents could provide unique stabilization effect on the formation of curved surface via DFT calculations so that quasi-continuous high-index microfacets could form. However, the understanding of curved surface of oxides is still in its infant and deserves urgent attention.

Herein, in this work, we demonstrate a facile organic-free hydrothermal strategy to fabricate unique microsized rutile TiO_2 crystals with a new type of curved surfaces by the synergistic effects of inorganic-inorganic capping agents and intriguingly, by solely altering the concentration of F^-, we could readily control the proportion of {110} facets. Moreover, we have revealed that the curved surfaces consist of nano-hills, which are different from the quasi-continuous curvature observed in the previous report[9].

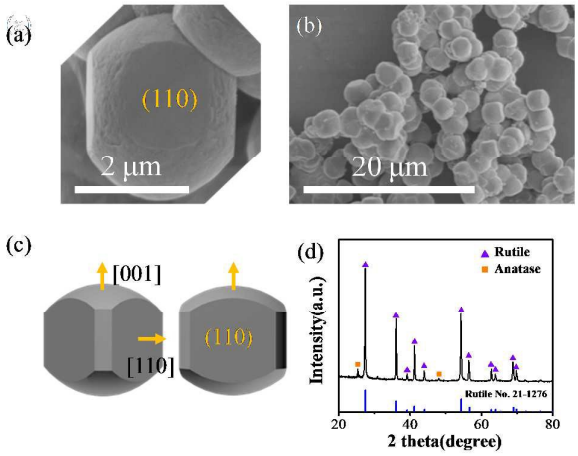

Fig. 1 (a-b) Typical SEM images, (c-d) schematic model and XRD pattern of the as-synthesized rutile TiO_2 single crystals synthesized with 8.5 μL HF.

The unique rutile TiO_2 single crystals were prepared by a facile organic-free hydrothermal synthesis in the presence of hydrofluoric acid and hydrochloric acid under extremely acidic conditions with titanium nitride as a starting material. In contrast to the prior examples of the faceted TiO_2 microcrystals[1, 18], representative scanning electron microscopy (SEM) images of the products reveal unconventional pillow-shaped crystals with curved surfaces as shown in Fig. 1(a) and (b). The displayed rutile single crystals are microsized with an edge to edge width (W) of ~2.6 μm, and an apex to apex length (L) of ~3.4 μm. Interestingly, they possess two curved apexes and four lateral smooth {110} facets which can be confirmed later by transmission electron microscopy (TEM) analysis in Fig. 2. It should be mentioned that although the rutile phase (JCPDS No.21-1276) is dominant, a small amount of anatase phase (JCPDS No.21-1272) can still be observed, as shown in the X-ray diffraction (XRD) pattern in Fig. 1(d). The phase contents of rutile and anatase in the products are determined via XRD pattern by use of an empirical equation (Eq.1, ESI†), from which we can roughly estimate that the weight fraction of rutile phase in the product is ~93.8%.

Center of Electron Microscopy and State Key Laboratory of Silicon Materials, School of Materials Science and Engineering, Zhejiang University, Hangzhou 310027, China. E-mail: yongwang@zju.edu.cn
† Electronic Supplementary Information (ESI) available. See
DOI: 10.1039/x0xx00000x
‡ These authors contributed equally to this work.

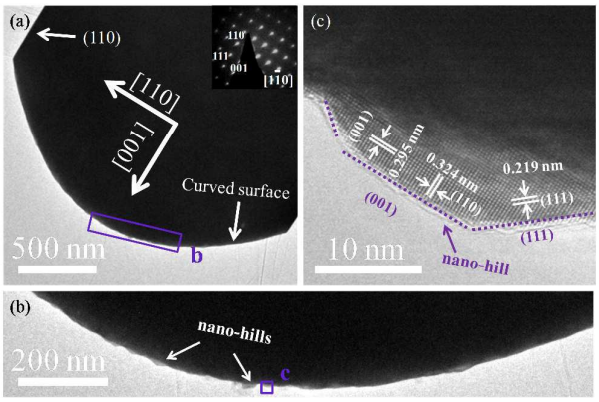

Fig. 2 (a) TEM image of a rutile TiO_2 single crystal synthesized with 8.5 µL HF viewed along the [1-10] zone axis. Inset: SAED pattern. (b) TEM image obtained from the purple rectangular area in (a). (c) HRTEM image recorded from the purple rectangular area in (b).

TEM/high-resolution TEM (HRTEM) images and selected area electron diffraction (SAED) pattern in Fig. 2 provide further insight into the microstructure of the synthesized crystals. Fig. 2(a) shows a low-magnification TEM image of a rutile TiO_2 single crystal and the corresponding SAED pattern, respectively. The SAED pattern (see the inset of the Fig. 2(a)) can be indexed to the [1-10] zone axis of rutile TiO_2. And Fig. 2(b) presents part of the novel curved surface, from which we see that the curved surface consists of nano-hills instead of quasi-continuous miller-index microfacets[9]. The HRTEM image in Fig. 2(c) acquired from the purple rectangular area in Fig. 2(b) shows the fringe spacing of 0.324 nm, 0.295 nm and 0.219 nm, which correspond to that of the {110} ,{001} and {111} planes of rutile titania, respectively, and the purple dotted line exhibits the outline of an individual nano-hill at the atomic scale, from which we see the nano-hills bound by high-energy {001} and {111} facets. It is obvious in Fig. 2 that curved surfaces of the TiO_2 particle have grown along the [001] direction and the four lateral facets are {110} facets. With regard to existing anatase phase, as shown in Fig. S1, it is revealed that these anatase nanosheets have single-crystal characteristics and the SEAD pattern can be indexed to [001] zone. Additionally, the HRTEM image in Fig. S1(b) clearly shows (200) and (020)atomic planes with a lattice spacing of 0.191 nm .

In the synthetic method, different from Yang's work[9], we controlled the morphology and polymorph of round rutile TiO_2 crystals via changing the amount of inorganic acid rather than adding various kinds of organic additives. In particular, we found that the ratio of {110} facets as well as the L/W ratio could be readily regulated by adjusting the concentration of HF when the other reaction conditions were set constant in the experiments. In fact, perfect TiO_2 particles with curved surface can only be obtained with a narrow range of HF amount. Without HF, only rectangular parallelepiped rutile TiO_2 nanorods were obtained in aggregated states (Fig. S2(a), ESI†). When the amount of HF added is increased to 30 µL, uniform antatase TiO_2 nanosheets with predominant {001} facets formed (Fig. S2(b), ESI†). Intriguingly, when we vary the amount of HF from 4.5 µL to 12.5 µL, it is clearly seen in the Fig. 3(a)-(c) that rutile particles with unique curved surfaces were prepared and that the {110} facets are gradually eliminated with the increase of the concentration of HF (see the schematic model in Fig. 3(d)). The crystal characteristics of elongated and compressed rutile crystals were confirmed using XRD patterns, TEM images and the SAED patterns (see details in Fig. S3 and S4, ESI†). With the addition of 4.5 µL HF, pillar-shaped elongated particles with a unique arc roof were obtained. In contrast, when the amount of HF was increased to 12.5 µL, elongated TiO_2 crystals were evolved into compressed pillow-shaped particles with a larger edge-to-edge width, suggesting that fluoride ions changed the growth rate of the facets of rutile single crystal and apparently, the growth rate along the [001] direction was decreased while that of the {110} facets was accelerated. It should be noted that along with the increase of HF, the mass fraction of anatase phase in the product increased as well (from 3.3 wt% at 4.5 µL to 19.7 wt% at 12.5 µL), indicating F^- played the key role for the phase transformation from rutile to anatase. It is well documented that the Ti-F bonds may inhibit the nucleation and growth of rutile TiO_2 and promote the formation of anatase[2, 19], while high concentration of HCl (~4.6 M in our experiment) in the reaction system is favorable for rutile formation[20]. And if one wants to obtain pure rutile phase, a higher concentration of Cl^- ions and high acidity are necessary.

To confirm the chemical states of F, Cl and N in the synthesized samples, high resolution X-ray photoelectron spectra were acquired and the results are shown in Figure 4(a)-(b) and Fig. S5-6 (see ESI†). The binding energy of F 1s core electrons is 684.3 eV (Fig. 4(a)), which belongs to the typical surface Ti-F species[1, 21, 22]. However, Cl 2p exhibits no peak at around 198.1 eV and 199.8 eV (see Fig. S5, ESI†, and Fig. 4(b)), which is identical to the results of Imai et al's[23] and Wu et al's[24] work. Wu and co-workers attributed this phenomenon to Cl's low adsorption energy due to their DFT theoretical calculation results. Though no Cl 2p signals appeared in the XPS results, it is well documented that Cl ions are favorable for rutile formation[27] and Cl ions tend to adsorb on the {110} facets of rutile[23, 25, 26], which further retards growth along the [110] direction. Anyway, more work is needed to uncover the reason of the "disappearance" of Cl from the XPS results. In regard to N, we found the presence of N atoms at the interstitial sites (Detailed discussion see Fig. S6, ESI†) and the products didn't show extra visible light adsorption which may be attributed to the interstitial-site nitrogen doping (Fig. S7, ESI†).

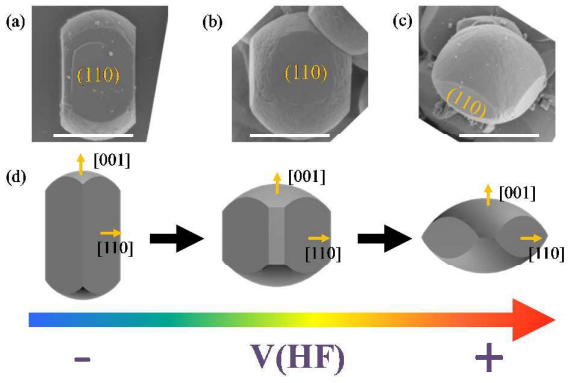

Fig. 3 Morphology (SEM) evolution (a)-(c) and corresponding geometric models (d) of rutile TiO_2 particles synthesized with different amounts of HF. All crystals were synthesized under the same conditions with 4.5 µL, 8.5µL and 12.5 µL HF. Scale bars are 2 µm.

To explain the formation mechanism of the curved surface of TiO_2, Yang et al.[9] proposed a model and they deemed that the continuous bending of the crystal surface could be attributed to the synergistic effects of chemisorbed organic–inorganic capping agents. For the rutile case, in particular, they claimed the curved surfaces were initiated at the high-energy (1-11) facets. For our as-prepared rutile TiO_2 crystals, as mentioned above, HF and HCl have played vital roles in the formation of curved rutile crystal surfaces and the control of crystal morphologies. To unravel the particular roles of

different capping agents (F and Cl), we performed first-principles DFT calculations on different rutile surfaces. In detail, the surface free energies of rutile (110), (001), (111)-ns, and (111)-s and (101) five facets terminated by X atoms were investigated, where X represented F and Cl. Note that two types of clean (111) facet may exist: one is nonstoichiometric facet ($Ti_{34}O_{72}$) (denoted as (111)-ns) and the other is stoichiometric surface ($Ti_{34}O_{68}$) (denoted as (111)-s). Fig. S8 and Fig. S9 (see ESI†) illustrates the models of clean and X-terminated rutile (110), (001), (111)-ns, (111)-s and (101) surfaces, respectively. Calculated energies of different surfaces adsorbed by X atoms are shown in Fig. 4(c), from which two conclusions can be drawn: among the five F-terminated surfaces, the (111)-s surfaces are most stable, though the differences among those four facets except (111)-ns are not significant; when covered by adsorbate Cl atoms, (110) facets yield the lowest value of γ, but the γ value is still higher than that of F-terminated (110) facets. These results indicate that we may regulate the proportion of (110) facets via varying the HF concentration and keeping HCl unchanged. Indeed, we successfully controlled the ratio of {110} facets by adjusting the amount of HF in our experiments, as shown in Fig. 3.

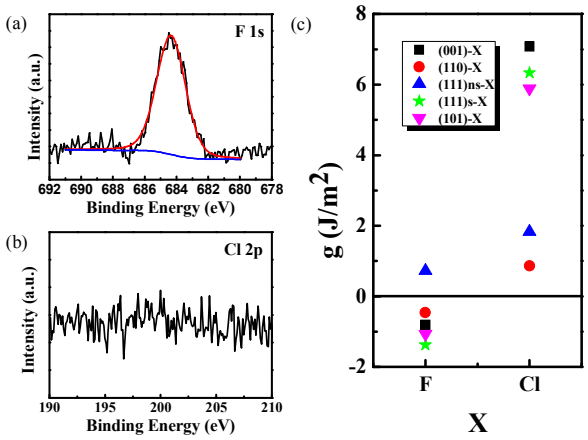

Fig. 4 High resolution XPS spectra of (a) F 1s and (b) Cl 2p of the rutile TiO_2 particles. The black lines are the raw data, and the blue and red lines represent the base line and fitted lines, respectively. (c) Calculated energies of (110), (001),(111)-ns, (111)-s and (101) surfaces surrounded by X atoms.

Also, according to the calculations, it might be possible to achieve rutile TiO_2 single crystals with a high percentage of (111) facets if their surfaces are ideally covered by F atoms, which is experimentally verified in a previous work done by Lai et al[18]. They achieved (111) facets using NaF as the capping agent and thought that the F–Ti species stabilized the high-energy (111) facets of rutile TiO_2. However, instead of flat (111) facets, curved surfaces were formed in our case in the temperature range from 160 °C to 180 °C, where a similar growth condition was employed except a lower temperature. This result allows us to believe that the growth temperature played an important role in the formation of such curved surfaces. Indeed, we obtained rutile TiO_2 with flat (111) facets by solely increasing the growth temperature in our experiments (see details in Fig. S10, ESI†). Intriguingly, similar phenomena were also reported in the rutile TiO_2 nanorods. It is revealed that those nanorods with exposed (111) surfaces only formed when the growth temperature is above 200 °C[27]. However, if the growth temperature is the only reason accounting for the formation of the curved surface, one might yield perfect curved surfaces on the top of rutile nanorods at a lower growth temperature. It is obviously not true as Zhang et al.[27] did so and only irregular and rough surfaces were obtained for the nanorods. Moreover, their work indicates that without the participation of F^-, curved surfaces would not form as their reaction system only contained Cl^-. Taking all these into consideration, we expect that the synergistic effect of F^- and Cl^-, a moderate temperature and a extreme acidic environment are responsible for the formation of such curved surfaces. Nevertheless, further experiments are required if one wants to get a deeper insight into this unconventional structure.

Finally, we demonstrate that such synthetic strategy can be also applied to other Ti precursor systems, such as tetrabutyl titanate (TBOT) and $TiCl_4$, to obtain titania single crystals with unique curved surfaces (Fig. S11, ESI†). These results indicate that this synthetic method may be a general way to fabricate curved surfaces by taking advantage of the synergistic effect of F and Cl ions.

In summary, rutile TiO_2 single crystals with novel curved surfaces and tunable lateral {110} facets were successfully synthesized through a facile organic-free hydrothermal method under the synergistic effect of F and Cl ions. It is revealed that the curved surfaces are not composed of quasi-continuous miller-index microfacets, but consisting of high-energy-facet-bound nano-hills. We have also demonstrated that the proportion of {110} facets and the aspect ratio could be regulated via solely altering the concentration of F^-. This organic-free synthetic strategy provides another solution for fabricating crystals with curved surfaces and may shed light on the deeper understanding of the formation mechanism of curved surfaces of functional semiconducting materials.

Acknowledgements

We acknowledge the support of National Science Foundation of China (51390474, 11234011, 11327901), the Ministry of Education of China (IRT13037) and National Young 1000 Talents Program of China. The authors thank Chenghua Sun at Monash University and Shengbai Zhang at RPI for helpful discussion.

References

1 H. G. Yang, C. H. Sun, S. Z. Qiao, J. Zou, G. Liu, S. C. Smith, H. M. Cheng and G. Q. Lu, *Nature*, 2008, **453**, 638-641.
2 G. Liu, H. G. Yang, J. Pan, Y. Q. Yang, G. Q. Lu and H.-M. Cheng, *Chemical Reviews*, 2014, **114**, 9559-9612.
3 K. Inoke, B. Freitag, A. B. Hungria, P. A. Midgley, T. W. Hansen, J. Zhang, S. Ohara and T. Adschiri, *Nano Letters*, 2007, **7**, 421-425.
4 X. Xie, Y. Li, Z.-Q. Liu, M. Haruta and W. Shen, *Nature*, 2009, **458**, 746-749.
5 M. Leng, M. Liu, Y. Zhang, Z. Wang, C. Yu, X. Yang, H. Zhang and C. Wang, *Journal of the American Chemical Society*, 2010, **132**, 17084-17087.
6 J. Z. Yin, Z. N. Yu, F. Gao, J. J. Wang, H. A. Pang and Q. Y. Lu, *Angewandte Chemie-International Edition*, 2010, **49**, 6328-6332.
7 X. Han, M. Jin, S. Xie, Q. Kuang, Z. Jiang, Y. Jiang, Z. Xie and L. Zheng, *Angewandte Chemie*, 2009, **121**, 9344-9347.
8 Z. W. Pan, Z. R. Dai and Z. L. Wang, *Science*, 2001, **291**, 1947-1949.
9 S. Yang, B. X. Yang, L. Wu, Y. H. Li, P. Liu, H. Zhao, Y. Y. Yu, X. Q. Gong and H. G. Yang, *Nature communications*, 2014, **5**, 5355.
10 F. Amano, T. Yasumoto, O. O. Prieto-Mahaney, S. Uchida, T. Shibayama and B. Ohtani, *Chemical Communications*, 2009, 2311-2313.
11 J. Li and D. Xu, *Chemical Communications*, 2010, **46**, 2301-2303.

12 M. Liu, L. Piao, L. Zhao, S. Ju, Z. Yan, T. He, C. Zhou and W. Wang, *Chemical Communications*, 2010, **46**, 1664-1666.
13 H. B. Jiang, Q. Cuan, C. Z. Wen, J. Xing, D. Wu, X. Q. Gong, C. Li and H. G. Yang, *Angewandte Chemie International Edition*, 2011, **50**, 3764-3768.
14 X. Zhao, W. Jin, J. Cai, J. Ye, Z. Li, Y. Ma, J. Xie and L. Qi, *Advanced Functional Materials*, 2011, **21**, 3554-3563.
15 X. Han, F. Zhou, L. Li and C. Wang, *Chemistry, an Asian journal*, 2013, **8**, 1399.
16 B. D. Sosnowchik, H. C. Chiamori, Y. Ding, J.-Y. Ha, Z. L. Wang and L. Lin, *Nanotechnology*, 2010, **21**, 485601.
17 J. S. Chen and X. W. D. Lou, *Chemical Science*, 2011, **2**, 2219-2223.
18 Z. Lai, F. Peng, H. Wang, H. Yu, S. Zhang and H. Zhao, *Journal of Materials Chemistry A*, 2013, **1**, 4182-4185.
19 H. Cheng, J. Ma, Z. Zhao and L. Qi, *Chemistry of Materials*, 1995, **7**, 663-671.
20 H. B. Yin, Y. Wada, T. Kitamura, S. Kambe, S. Murasawa, H. Mori, T. Sakata and S. Yanagida, *Journal of Materials Chemistry*, 2001, **11**, 1694-1703.
21 G. Liu, H. G. Yang, X. Wang, L. Cheng, J. Pan, G. Q. Lu and H.-M. Cheng, *Journal of the American Chemical Society*, 2009, **131**, 12868-12869.
22 J. C. Yu, J. G. Yu, W. K. Ho, Z. T. Jiang and L. Z. Zhang, *Chemistry of Materials*, 2002, **14**, 3808-3816.
23 E. Hosono, S. Fujihara, K. Kakiuchi and H. Imai, *Journal of the American Chemical Society*, 2004, **126**, 7790-7791.
24 L. Wu, B. X. Yang, X. H. Yang, Z. G. Chen, Z. Li, H. J. Zhao, X. Q. Gong and H. G. Yang, *CrystEngComm*, 2013, **15**, 3252-3255.
25 B. Liu and E. S. Aydil, *Journal of the American Chemical Society*, 2009, **131**, 3985-3990.
26 Q. Huang and L. Gao, *Chemistry Letters*, 2003, **32**, 638-639.
27 H. Zhang, X. Liu, Y. Wang, P. Liu, W. Cai, G. Zhu, H. Yang and H. Zhao, *Journal of Materials Chemistry A*, 2013, **1**, 2646-2652.

